HYDROACOUSTICS
4, 109-118 (2001)

HIGH INTENSITY ULTRASOUND WAVES FROM A STRONGLY FOCUSED CIRCULAR SOURCE

Tomoo KAMAKURA and Masahiko AKIYAMA

The University of Electro-Communications
1-5-1, Chofugaoka, Chofu-shi, Tokyo 182-8585, Japan
e-mail address : kamakura@ee.uec.ac.jp

To verify the effectiveness of the spheroidal beam eguation (SBE) [J.Acoust. Soc.Am. 107, 3035-3046 (2000)] that is promisingly applicable to a theoretical pre-diction of strongly focused nonlinear beams, experiments arę carried out in water using a 1.6MHz focused transducer with a circular aperture of 73mm in diameter and a f ocal length of 75mm. The aperture half-opening angle becomes 29°, which exceeds the upper limit of the applicability of the KZK model eguation. At the max-imum, peak pressure attains about lOMPa at thefocus. For such intense waves, the pressure levels of the first three harmonics arę in fairly good agreement with the the-ory. The focused source is highly excited by a sinusoidal tone-burst signal with three periods to study nonlinear propagation of an ultrasonic pulse. For such a transient wave, the SBE theory agrees well with experiments. Significant distortion appears in the direct wave than the edge wave in the post-focal region, in particular, for the wave passing through a sheet of silicone rubber near the focus.

1. INTRODUCTION

Focused ultrasound has many applications to modern engineering such as medical diagnosis and non-destructive testing of materials. In particular, strongly focusing sources are frequently used to achieve high lateral resolution in ultrasonic imaging systems and high ultrasonic power at a localized spot, a focus, in industrial technologies. Since the amplitude of the sound emitted from such focusing sources increases abruptly with propagation toward the focus, waveform distortion may occur due to the inherent nonlinearity of the medium, even if the source pressure level is relatively low.

Quite a number of articles have been published on theoretical investigations of focused nonlinear sound beams. Almost all the works begin with the Khokhlov-Zabolotskaya-Kuznetsov (KZK) equation [1] that has been widely used as a model equation of finite-amplitude sound beams propagating in viscous nonlinear fluids. As Naze Tjotta *et al.* point out, however, the aperture half-angle of a focused source should be 16° or less for reliable parabolic or paraxial approximation, quite independent of focusing gain and ka, where k is the wavenumber and a is the aperture radius. This result is very important: we can not safely

use the parabolic equation and thus the reduced KZK equation to theoretically predict focusing beams from a wide aperture whose half-angle exceeds 16°.

In order to develop a pertinent model equation for strongly focused intense beams, Ystad and Berntsen [2] proposed the composite method (CM) that described the focused field in terms of two beam equations. One of them was the mixed model equation and was accurate close to the source and inaccurate approaching the focus. The other was the KZK equation that was accurate in the paraxial region, especially near the focus. The two equations presented in different coordinates were appropriately connected along a curve in an azimuth plane using the bi-cubic spline interpolation to determine the solution uniquely. They gave various numerical examples for on-axis profiles and beam patterns of the first few harmonic components. The aperture angle was set to 26.75° for comparison with their underwater experiments. However, experimental data for nonlinear sound propagation of the second and higher harmonics outside the domain of validity of the KZK equation were not available.

As an approach conceptually identical to the CM, we proposed a new model equation, the spheroidal beam equation (SBE), to describe the nonlinear focused beams from a circular aperture. A crucial difference from the CM is the use of an oblate spheroidal coordinate system, which is like the rectangular coordinates near the focus and is like the spherical coordinates near the source. The numerical interpolations Ystad and Berntsen have adopted are no longer needed to combine two model equations at a certain transition location; we can smoothly transfer from the spherical to plane wave domains by a simple connector. Even at an aperture half-angle of 40°, the peak amplitude of the sound pressure near the focus has almost the same magnitude as predicted by O'Neil.

As a whole, predicting harmonic generation from wide apertures and comparing theory and experiment in detail seem to still be lacking for aperture angles exceeding 30°. In order to examine harmonic generation in more detail, the present report concentrates on studying nonlinear behavior of strongly focused beams in the prefocal region, through the focus, and in the post-focal region. First, we summarize the model equation or SBE to provide a mathematical background. Next, we compare measured harmonic components in a CW finite-amplitude sound beam emitted from a 29° focusing source with those predicted by the SBE numerical solutions. Finally, some experimental results and their numerical simulations of pulse waves of finite amplitude are provided. The interesting features of the pulse changes in waveforms in the post-focal region are discussed.

2. SPHEROIDAL BEAM EQUATION

Having already described the theoretical foundations of the spheroidal beam equation (SBE) in detail [4,5], we only summarize this model equation here.

Figure 1 shows the oblate spheroidal co-ordinate system. Additionally, the geometry of an axisymmetric, concave-type sound source is given with focal length d, aperture radius a, and aperture half-angle $\alpha_0 = \sin^{-1}(a/d)$. On the assumption that the wave-length is much smaller than the focal length and the linear impedance relation of a plane progressive wave holds approximately in describing nonlinear source terms in the hydrodynamic equations, we have derived the spheroidal beam model equation. It is numerically demonstrated that the latter assumption is almost valid in a strongly focusing system whose aperture half-angle is up to at least 30° [4].

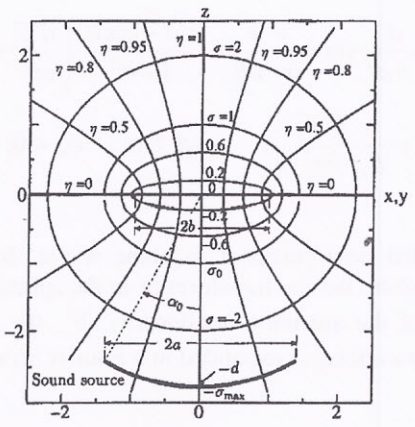

Fig. 1. Concave-type focusing source with apereture diameter 2a and focusing length *d*. η is cos θ.

The SBE is expressed in the spherical wave region of $\sigma < \sigma_0 < 0$ as

$$\frac{\partial^2 \overline{p}}{\partial \tau_s \partial \sigma} + \frac{1}{2}\frac{\sin 2\theta}{\sigma(1+\sigma^2)}\frac{\partial^2 \overline{p}}{\partial \tau_s \partial \theta} + \frac{\varepsilon\sqrt{\sigma^2+\sin^2\theta}}{\sigma(1+\sigma^2)}\left(\frac{\partial^2 \overline{p}}{\partial \theta^2} + cot\theta\frac{\partial \overline{p}}{\partial \theta}\right)$$
$$+\frac{E}{\sigma}\frac{\partial \overline{p}}{\partial \tau_s} = -\frac{\sqrt{\sigma^2+\sin^2\theta}}{\sigma}\left(\alpha b\frac{\partial^3 \overline{p}}{\partial \tau_s^3} + \frac{b}{2l_D}\frac{\partial^2 \overline{p}^2}{\partial \tau_s^2}\right)E \quad (\sigma < \sigma_0 < 0) \tag{1}$$

where the spatial variables σ and θ are related to the cylindrical coordinates *(r, z)* by

$$r = b\sqrt{(1+\sigma^2)}\sin\theta, \qquad z = b\sigma\cos\theta \tag{2}$$

with

$$0 \le \theta \le 90^o \tag{3}$$

2b is the interfocal length and is chosen to be smali compared to the aperture diameter *2a* for a large aperture source, r_s is the retarded time for spherical waves, sound pressure *p* is normalized as $\overline{p} = p/p_0$ with its initial amplitude p_0 at the source, $\alpha = \delta\omega^2/2c_0^3$ is the sound attenuation coefficient, and $l_D = \rho_0 c_0^3/\beta p_0 \omega$ is the shock formation distance for a plane wave. Moreover, ω is the angular frequency of ultrasound, ρ_0 is the medium density, c_0 is the small amplitude sound speed, β is the nonlinearity coefficient of the medium, and $\varepsilon = l/2kb$ (*k* the wavenumber). In general, $kb >> 1$, then $\varepsilon < 1$. *E* in eq. (1) is a function of σ and θ:

$$E(\sigma, \theta) = \frac{\sigma^2 + \cos^2\theta}{1+\sigma^2} \tag{4}$$

In the paraxial region, the SBE is expressed in another form as follows:

$$\frac{\partial^2 \bar{p}}{\partial \tau_p \partial \sigma} - \frac{\sigma}{1+\sigma^2}\sin\theta \frac{\partial^2 \bar{p}}{\partial \tau_p \partial \theta} - \frac{\varepsilon(2-\cos\theta)}{1+\sigma^2}\left(\frac{\partial^2 \bar{p}}{\partial \theta^2} + cot\theta \frac{\partial \bar{p}}{\partial \theta}\right)$$
$$= \left(\alpha b \frac{\partial^3 \bar{p}}{\partial \tau_p^3} + \frac{b}{2l_D}\frac{\partial^2 \bar{p}^2}{\partial \tau_p^2}\right) E \qquad (\sigma \geq \sigma_0, \quad \sigma_0 < 0) \tag{5}$$

where τ_p is the retarded time pertinent to plane waves. In eqs. (1) and (5), σ_0 is a specific transition location, where we can transform from the spherical to plane wave regions.

Due to the existence of the quadratic nonlinearity $\bar{p}^2$, the wave shape distorts during propagation. The distorted -waveform is expanded in a Fourier series:

$$\bar{p} = \begin{cases} \sum_{n=1}^{\infty} (g_n^{(s)} \sin n\tau_s + h_n^{(s)} \cos n\tau_s) & (\sigma < \sigma_0 < 0) \\ \sum_{n=1}^{\infty} (g_n^{(p)} \sin n\tau_p + h_n^{(p)} \cos n\tau_p) & (\sigma \geq \sigma_0, \sigma_0 < 0) \end{cases} \tag{6}$$

here $g_n^{(s)}$, $h_n^{(s)}$, $g_n^{(p)}$ and $h_n^{(p)}$ are the Fourier coefficients. Substitution of eq. (6) into eqs. (1) and (5) yields two sets of coupled and nonlinear partial differential equations for the Fourier coefficients. These equations seem too intractable to solve. However, numerical analysis using a finite difference scheme enables us to obtain readily the solutions of the n-th harmonie component.

Boundary conditions must be appropriately specified at the source face and at the transition juncture σ_0. The former conditions are imposed as

$$\bar{p}\big|_{\sigma=-\sigma_{max}} = \begin{cases} F(\theta)\sin\tau_s & \theta \leq \theta_0 \\ 0 & \theta > \theta_0 \end{cases} \tag{7}$$

where $\sigma_{max} = d/b$ denotes the focal length on the σ axis, and $F(\theta)$ is a pressure distribution function on the source. When the pressure amplitude is uniformly distributed, $F(\theta) = 1$. Angle θ_0 depends on the aperture angle α_0 and the focal length σ_{max}:

$$\theta_0 = tan^{-1}\left(\frac{tan\,\alpha_0}{\sqrt{1+1/\sigma_{max}^2}}\right) \tag{8}$$

The difference between α_0 and θ_0 is generally small. For example, when $\alpha_0 = 30°$ and $\theta_{max} = 10/3$, θ_0 becomes 28.94°, a little smaller than α_0.

We have to specify explicitly the boundary condition at the juncture to obtain a unique solution of the n-th harmonic in the region $\sigma > \sigma_0$:

$$g_n^{(p)} = g_n^{(s)} \cos\gamma - h_n^{(s)} \sin\gamma$$
$$h_n^{(p)} = g_n^{(s)} \sin\gamma + h_n^{(s)} \cos\gamma \qquad (at\ \sigma = \sigma_0 < 0) \tag{9}$$

here $\gamma = nkb\left(\sqrt{\sigma_0^2 + \sin^2\theta} + \sigma_0 \cos\theta\right)$.

Artificial sound reflections from the open boundary at θ = 90° may occur during wave propagation. In actual computation, a flow relaxation scheme [6] is utilized to minimize these reflections.

3. EXPERIMENTS AND DISCUSSION

The ultrasonic source fabricated by TOKIMEC Inc. is a focusing transducer with a l.GMHz fundamental resonant frequency and a circular aperture (Fig. 2). Focusing is achieved by cutting PZT materials in the form of a spherical concave surface. The effective aperture diameter is 73mm, and the geometrical focal length is 75mm. The half-angle of the aperture then becomes $\sin^{-1}(38/75) \approx 29°$. The source. immersed in fresh and degassed water, which was driven by a 300W RF power amplifier, was radiating tone-burst sinusoidal waves of about 50 cycles duration to avoid reflection from the walls of a rectangular tank. The burst waves emanating from the center and edge of the source overlapped fully to establish a steady-state condition within the range of 55mm to l00mm from the center of the source face. The water temperature was about 26°C, then the sound speed and sound absorption coefficient were estimated to be 1500m/s and $21.2 \cdot 10^{-15} f^2$ neper/m, respectively, where f is frequency in Hz.

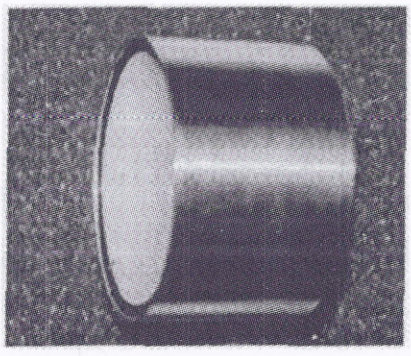

Fig. 2. Ultrasound transducer

A NTR card-type PVDF hydrophone with a very small sensing area of 0.2 × 0.2mm was used to pick up local sound pressure and was mounted on a translation stage driven by stepping motors. The motors enabled the stage to move precisely along and across the acoustic axis in steps as smali as lμm. The output signals from the hydrophone were captured using a LeCroy digital storage oscilloscope (DSO) with a 100MHz sampling rate and 8-bit digitizing resolution. The motors and the DSO were both controlled by a per-sonal computer. An alternative task for the oscilloscope was to determine the frequencies of the received signals using the built-in FFT analyzer.

It is of great interest to compare quantitatively the SBE model with the transformed KZK equation model. Figure 3 shows numerical solutions based on each model equation and experimental data for the first three harmonics. In all figures, solid and dashed curves are the solutions using the SBE and the KZK equation, respectively. Dotted curve in the fundamental components (top figure) is the linear theory (0'Neil's formula).

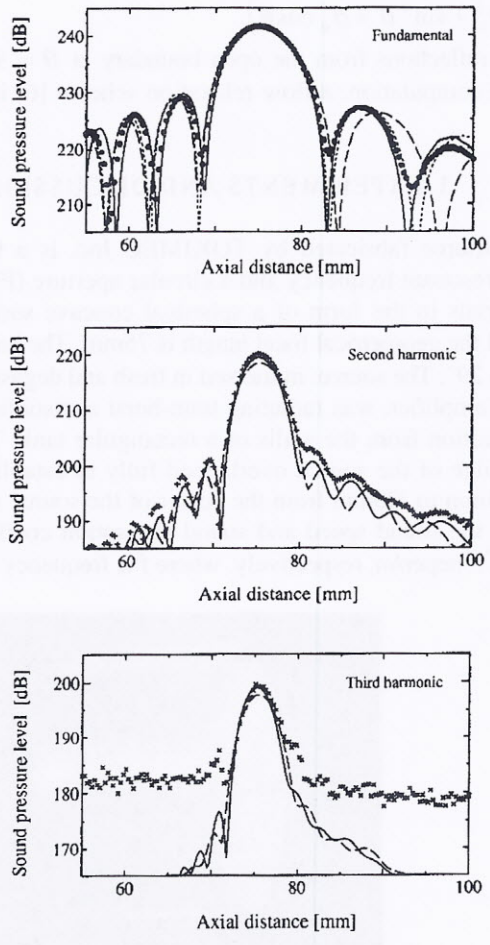

Fig. 3. Companson between the measured pressure amplitudes (symbols) and theoretical predictions (lines). *po* = 27.9kPa. • fundamental, + second harmonic, × third harmonic, — SBE, - - - transformed KZK equation, - - - O'Neil's formula (fundamental components only).

We note that the experimental results are overall in good agreement with the solutions by the SBE rather than those by the transformed KZK equation. In particular, there are similarities in the oscillatory pressure curves between the experiment and the SBE simulation. Moreover, the peak pressure levels of the second and third harmonics predicted by the transformed KZK equation are two or three decibels lower than those by the SBE. Incidentally, numerical parameters for the KZK equation are as follows :

$$u_{\max} = \frac{2.5}{1+\delta}, \quad \delta = 10, \quad \Delta u = \frac{u_{\max}}{1900}, \quad \Delta\sigma = 0.3G(\sigma\pm\delta)^2(\Delta u)^2 \qquad (10)$$

The notations listed are the same as those Hart and Hamilton [7] have employed. The parametric gain, G, becomes 59.2 in the present focusing system. Moreover, the normalized axial distance σ corresponds to ζ in the notations used in the SBE model. It takes about 10 times longer to finish computation in the transformed KZK equation compared with the SBE when numerical parameters such as the harmonie number are the same.

Sound pressure levels at the focus were measured by changing the yoltage applied to the transducer. Figure 3 shows the results, where 0dB in the abscissa corresponds to on-source pressure amplitudę p_0 = 27.9kPa. It was theoretically assumed that p_0 is linearly proportional to the source voltage. At the maximum input level of 21dB (on-source pressure amplitudę is theoretically 313kPa), 150 harmonics were retained in calculation to obtain the fundamental to the third harmonics. Surprisingly, the fundamental pressure level reaches 261dB in this source condition.

Comparison between the measured response curves and the corresponding theoretical curves shows a good agreement for each harmonie component. However, there can be seen some discrepancies in the data of the third harmonie below 0dB owing to poor digitizing resolution of the DSO. An 8-bit digitizer has a dynamic range of 42dB at best. Indeed, the difference in levels between the fundamental and third harmonic pressures is about 42dB. Unfortunately, measurements are restricted to the range up to 14.5dB (p_0 = 148kPa) since the linearity of the power amplifier breaks down for higher voltage excitation.

By inspecting that the theoretical response curves shown in Fig. 3 begin to bend over gradually around 15dB, we can predict that nonlinear absorption occurs significantly above that level. Strong nonlinear absorption due to shock formation must induce acoustic saturation and beam broadening. These nonlinear effects come out in finite-amplitude beams from a planar unfocused source as well. As Hart and Harnilton say [7], however, the onset of the nonlinear absorption in strongly focused beams is far less insensitive to source pressure than that in unfocused beams.

4. FINITE-AMPLITUDE PULSE PROPAGATION

Up to this point we have verified the use-fulness of the SBE model in describing a finite- amplitude CW from a strongly focusing source, so we next present some numerical and experimental examples of nonlinear propagation of a focusing pulse. The present demonstration emphasizes the waveform distortions of the pulse during propagation due to nonlinearity and diffraction. For wide-angle apertures, a strong nonlinear interaction occurs substantially in a limited region near the focus. The pulse waveforms may thus change markedly when they are passing through the focus.

The initial wave of interest here is a sinusoidal pulse consisting of several cycles. Two emitted waves, the direct pulse that comes from the center of the source and the diffracted pulse that comes from the edge, are sufficiently separable in time except for the focus region. The former pulse arrives ahead of the latter pulse in the pre-focal region, and *vice versa* in the post-focal region. We can therefore investigate how the nonlinear interaction of the two pulse affects wayeform distortion. As a rule, a large number of harmonics must be retained, requiring much computation time. Here, however, a straightforward numerical algorithm based on a Fourier series expansion was utilized to obtain the steady-state solutions of the SBE [5].

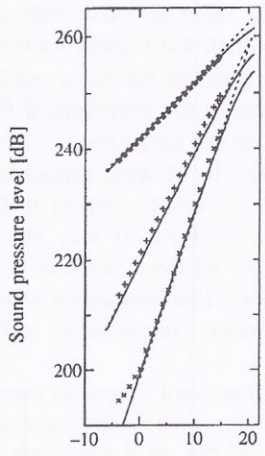

Fig. 4. Pressure amplitudes at the focus as a function of the source pressure p_0. • fundamental, + second harmonic, × third harmonic, — SBE solution, - - - p_0^n -dependence straight lines in a full logarithmetic scale (n is the n-th narmonic)

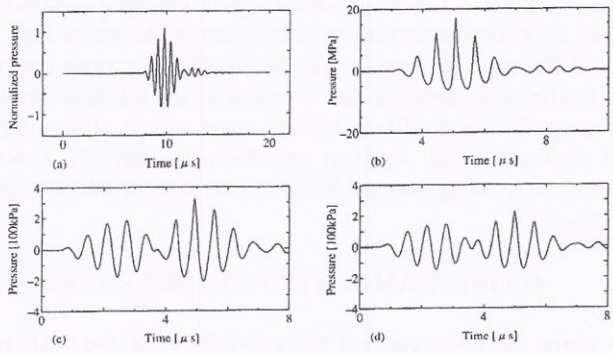

Fig. 5. On-axis waveforms of the finite-amplitude pulse. Initial waveform(a), theoretical waveform at the focus(b), theoretical waveform at z = 121mm, and experimental waveform at z = 121mm. p_o = 150kPa.

Waveforms changes during propagation are seen in Fig. 5, where the curve (a) is the initial source signal theoretically derived from the measured waveform at the focus. When the source excitation is low so as not to generate great distortion, the linear relationship between the waveforms at the source and at the focus holds:

$$p(t')\Big|_{at\ focus} = \frac{a}{c_0} tan\left(\frac{\alpha_0}{2}\right)\frac{d}{dt}\, p(t')\Big|_{on\ source} \tag{11}$$

where $t' = t - z/c_0$ [8]. The initial signal $p(t')\,|_{\text{on source}}$ for numerical computation is readily obtained by integating eq. (11) with respect to time. Owing to inappropriate damping, a small ringing signal appears after the main signal.

The curve (b) shows the theoretically obtained focal waveform. The repetition frequency is 50kHz, and 640 harmonics are retained in the computation. At the focus, a distorted pulse is associated with the coalesced portion of the direct and diffracted waves for the high

source pressure alone. The diffraction-induced asymmetry of the peak positive pressure, which is considerably sharper than the negative trough, is manifested. The positive peak reaches 17MPa, which is almost twice the negative pressure —7MPa.

After passing through the focus, the diffacted pulse is ahead of the direct pulse and their polarities are reversed. The waveform (c) is the theory at z = 121mm in the post focal region, 46mm away from the focus. The first arrival pulse in the figure is the edge wave, and the second the direct wave. They are almost separated on the time axis. As can be seen, the magintude of the direct wave is about 20% greater than that of the edge wave. Additionally, noticeable distortion appears in the direct wave, although it is not remarkable. Experimentally observed waveform at the same position is given in the curve (d). It is noted that the theory overestimates slightly the pressure magnitude of the direct wave.

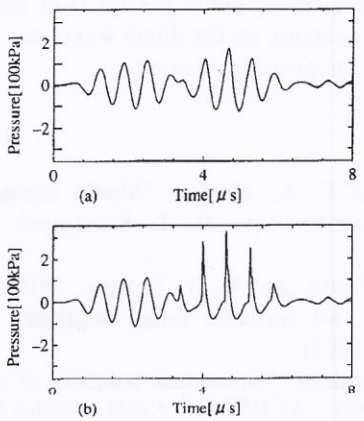

Fig. 6. Experimentally observed waveforms at z = 121mm. A sheet of silicone rubber in thickness5mm is inserted at z = 60mm (a) and z = 75mm (b), respectively.

Hobæk and Ystad [9] investigated strong shock formation in highly intense focusing beams from a CW ultrasound source theoretically and experimentally. They concluded that there is an appropriate connection between the shock wave and the signal wave generated near the edge of the source. Furthermore, they said that the shock may be associated with the direct wave, and the signal wave, which they called the back-ground signal, is mainly associated with the edge wave. The present theory and experiment indicate, in principle, the same results as Hobæk's prediction, i.e., the shock in the post-focal region depends primarily on the direct wave.

(Striking distortion is experimentally observed in the direct wave by inserting a sheet of silicone rubber at the focus. The sheet thickness is 5mm and is wide enough to transmit fully both the direct and edge waves. Sound pressure signals are picked at z = 121mm on the axis, the same position as in Fig. 5 (c) and (d). Figure 6(b) shows the results, where for comparison the waveform is given in the curve (a) when the rubber sheet is placed at z = 60mm in the prefocal region. The first pulses in both the waveforms have almost the same in their magnitude and shapes. However, the second pulses differ greatly in shape : spike-like pulses are generated in the direct wave. It is found that the nonlinearity of the rubber is about 7 times greater than that of the water [10], then nonlinear distortion is apt to generate significantly in the wave passing through the rubber.

5. CONCLUSION

Sound pressure amplitudes from the fundamental to third harmonie were measured in water for a l.GMHz, finite-amplitude, CW emitted from a focused source with a focal length of 75mm and a circular aperture of about 73mm in diameter. Since the aperture half-angle of 29° exceeded the applicability criteria of the KZK equation, the spheroidal beam equation (SBE), which is useful for field analysis of ultrasound beams emitted from a concave focusing source with a wide-angle aperture, was used to theoretically predict harmonic generatation. Overall, experimental results agree well with theoretical results.

Some numerical and experimental examples of intense sound pulses emitted from a wide aperture demonstrated that the coalesence of the direct and edge waves in the focal region generates spike-like wavefronts, in particular, in the pulse passing through a sheet of silicone rubber whose nonlinearity is much greater than the water's. It is demostrated that such peculiar spikes remain parasitic on the direct wave, not on the edge wave, even after the two waves have separated in the post-focal region.

REFERENCES

1. M. F. Hamilton and C. L. Morfey, "Model equations," in *Nonlinear Acoustics,* edited by M. F. Hamilton and D. T. Blackstock (Academic Press, Calif.,1998), Chap.3.
2. J. Naze Tjotta, S. Tj0tta, and E. H. Yefring, "Effects of focusing on the nonlinear inter-action between two collinear finite amplitudę sound beams," J. Acoust, Soc. Am. 89, 1017-1027 (1991).
3. B. Ystad and J. Berntsen, "Numerical solution of parabolic equations for strongly curved focusing sources," ACUSTICA • acta acustica 82, 698-706 (1996).
4. T. Kamakura, T. Ishiwata, and K. Matsuda," Model equation for strongly focused finite-amplitude sound beams," J.Acoust.Soc.Am. 107, 3035-3046(2000).
5. T. Kamakura, K. Aoki, and T. Ishiwata, "Nonlinear propagation of focused ultrasound beams from a wide-angle aperture,"ACUSTICA • acta acustica 86, 446-456 (2000).
6. B. Ystad and J. Berntsen, "Numerical solution of the KZK equation for focusing sources," acta acustica 3, 323-330(1995).
7. T. S. Hart and M. F. Hamilton," Nonlinear effects in focused sound beams," J.Acoust.Soc.Am. 84, 1488-1496 (1988).
8. M. F. Hamilton, "Comparison of three transient solutions for the axial pressure in a focused sound beam," J. Acoust. Soc. Am. 92, 527-532 (1992).
9. H. Hobæk and B. Ystad," Experimental and numerical investigation of shock wave propagation in the post focal region of a focused sound field," ACUSTICA • acta acustica 83, 978-986 (1997).
10. J. D. Ryder, P. H. Rogers, and J. Jarzynski,"Radiation of difference-freqeuncy sound generated by nonlinear interaction in a silicone rubber cylinder," J. Acoust. Soc. Am. 59, 1077-1086 (1976).